International Journal of
Geohazards and Environment
http://ijge.camdemia.ca, ijge@camdemia.ca

IJGE 2016 2(3): 104-118
Available at http://ojs.library.dal.ca/ijge

Quantitative Estimations of the Holocene Erosion due to Seismically Induced Landslides in the SE Altai (Russia) Applying Detailed Profiling and Statistical Approaches

Roman Nepop[1, 2*], Anna Agatova[1, 2]
[1] Sobolev Institute of Geology and Mineralogy, Koptyuga Avenue, 3, Novosibirsk, 630090 Russia
[2] Ural Federal University, Yekaterinburg, Mira Street, 19, 620002 Russia

Abstract: Earthquakes are some of the most disastrous natural hazards. Coseismic slope failures often significantly contribute to the global damage and may cause most of the casualties related to strong earthquakes. Seismically induced landslides are widespread phenomena within tectonically active mountain terrain. Their abundant occurrence and the large volumes of displaced slope material reveal their great influence on topographic changes. This paper presents new correlations between the earthquake magnitude and the total volume of displaced slope material and between earthquake magnitude and the volume of the largest triggered landslide. These relationships allow us to quantify erosion due to seismically triggered landslides. Calculation of the total volume of displaced slope material is based on the parameters of the largest landslides which could be preserved in the topography for thousands years. This approach was tested in the most seismically active southeastern part of Russian Altai, which is evidenced by numerous giant earthquake-induced paleo-landslides. The total volume of slope material displaced during ancient earthquakes within the Chagan-Uzun river basin, calculated on the basis of statistical correlations, is $(3.0\text{-}4.3)\times10^{-1}$ km^3, and the Holocene erosion rate due to seismically induced landslides $(1.1\text{-}3.0)\times10^{-5}$ m a^{-1}. The numerical estimates were verified by calculating the volumes of all detected earthquake-triggered landslides within the Chagan-Uzun river basin and the neighboring Kurai basin on the basis of detailed profiling approach, which are 1.33×10^{-1} and 2.25×10^{-1} km^3, respectively. The Holocene erosion rate due to seismically induced landslides in these basins could be estimated at 1.1×10^{-5} and 1.4×10^{-5} m a^{-1}, respectively. Thus the Holocene erosion rate of the SE Altai due to earthquake-triggered landslides obtained by applying different techniques can be estimated at $(1.1\text{-}3.0)\times10^{-5}$ m a^{-1}, which more precisely characterizes topography changes within the Chuya-Kurai system of intermountain depressions and framing ridges.

Keywords: seismicity, paleoseismogeology, earthquake-triggered landslides, erosion rate, detailed profiling, Russian Altai, Holocene

1 Introduction

Seismically triggered landslides accompanying strong earthquakes are one of the most dangerous natural hazards. Coseismic slope failures, which are widespread phenomena within tectonically active mountain terrain, represent a high risk to both human lives and construction. Numerous examples provide evidence for this. The well-known catastrophic Huascaran rock debris avalanche triggered by the 1970 Peru earthquake (M=7.7) killed more than 18,000 people (Plafker et al 1971); giant loess landslides induced by the 1920 Haiyuan earthquake, NW China, (M=8.5) caused about 100,000 casualties (Schuster and Highland 2001); and a long run out loess and rock

* Corresponding Author: Roman Nepop, agatr@mail.ru, Tel: +7 (383) 330-8363

DOI: 10.15273/ijge.2016.03.012

avalanches triggered by the 1949 Khait earthquake (M=7.4) (Havenith et al 2015) destroyed local settlements in the Yasman valley and buried Khait town with thousands of inhabitants.

Seismically triggered landslides are also especially important agents of denudation in tectonically active zones. Each strong earthquake can cause thousands of seismo-gravitational deformations with a total volume of displaced slope material of several millions of cubic meters within an area of thousands of square kilometers (Keefer 1994, Keefer and Wilson 1989). In some regions, erosion due to seismically triggered landslides reaches up to 50% of total topographic denudation (Keefer 1994). In spite of diversity in climatic, geological, geomorphological conditions and peculiarities of seismic process for different areas, landslides of various types can be triggered even by moderate seismic shocks with the smallest magnitudes of approximately 4 – 5 (Keefer 1994, Bommer and Rodriguez 2002). Since about 1/5 of the Earth's surface is affected by earthquakes, evaluating of seismic risk hazard and associated topography changes is a matter of vital importance.

Accompanying the process of mountain growth, more intensive erosion is related to periods of increased tectonic activity and relief sharpening. The practically instant impact of seismically triggered mass wasting slope processes on topography can be equivalent to long term (hundreds and even thousands years) effects of other erosional agents (Iveronova 1969). Despite the fairly detailed documentation of large earthquake-triggered landslides, the influence of seismically induced slope processes on erosion is still poorly investigated. The main problem of calculating erosion due to earthquake-triggered landslides is the complexity of quantifying the volume of rocks displaced from the slopes during seismic shocks. Although sedimentary records could indicate the periods of tectonic activity due to the increasing size of deposited colluvial debris, these records cannot solve the problem of estimating the influence of seismically triggered landslides on denudation as well as its comparison with other erosional agents, such as glaciers and rivers. The determination of seismically displaced slope material deposited in piedmont foredeeps and even in intermountain depressions is practically impossible. Often even high mountainous lacustrine sedimentary archives don't contain information about catastrophic topography changes associated with seismic events. Such sedimentation records more sensitively reflect moisture fluctuation (Kashiwaya et al 2004). Slope material displaced as a result of recent Holocene earthquakes may not reach the local erosion base level (usually associated with floors of intermountain depressions) and is accumulated within mountain valleys. This is the reason why quantifying the volume of earthquake triggered landslides through a statistical approach and through the profiling method are currently the most exploitable techniques worldwide. Obviously utilizing both techniques gives the opportunity to estimate the volumes of displaced strata and the related erosion due to seismically induced landslides for the last 10 - 15 ka, only. During this time period the largest landforms could be preserved under arid climate conditions. The lifespan of such landforms in humid climate is significantly smaller. In this case, the largest landslide triggered by an earthquake is the most interesting target for paleo-seismogeological investigations for several reasons. First of all, it leaves the most persistent imprint on landforms and thus represents the longest period of seismic activity. Then, our data on strong modern and prehistoric earthquakes for the Altai-Sayan mountain province show that the volume of the largest landslide is several times or even orders of magnitude greater than the volume of the next one. Thus each largest landslide is related to a separate trigger unlike faults or smaller landslides. And finally, large landslides can be well identified from remote sensing imagery which is especially important for hardly accessible terrain.

In this paper we develop previously presented approach of estimating paleoseismicity and earthquake-induced topography changes (Nepop and Agatova 2008, Agatova and Nepop 2009, Agatova and Nepop 2011). In addition to previously specified correlation between earthquake magnitude and the total volume of slope material displaced as a result of this

earthquake (Nepop and Agatova 2011), we present a correlation between earthquake magnitude and the volume of the largest triggered landslide and three independent equations for calculating the total volumes of seismically triggered landslides. This approach gives an opportunity to utilize parameters of the largest seismically induced landslides for quantifying erosion, and expands the scope of classical paleoseismogeological method (Solonenko 1973). So far within the frame of this method seismically induced landslides have been used mainly for establishing epicentral zones and possible timing of past earthquakes (Solonenko 1962, 1973).

2 Methods of Quantifying Erosion due to Seismically Induced Landslides

The quantitative assessment of earthquake-induced topography changes can be done using V_{LT}, the volume of landslides triggered by single seismic event. This value defines the destructive effect of earthquake resulting in topography changes. The intensity of these changes can be evaluated by the erosion rate due to seismically induced landslides $\dot{h}$ (Nepop and Agatova 2011):

$$\dot{h} = \alpha \times \frac{\sum V_{LT}}{S \times T} \quad (1)$$

Here $\sum V_{LT}$ is a total volume of all landslides triggered by each individual earthquake, summarized for all strong earthquakes within a region with the surface area S during time period T; α is the regional factor taking into account the contribution of aftershock-triggered landslides (Agatova and Nepop 2009). For an accurate estimate, all strong earthquakes over this time period should be taken into account. Moreover, T should be much longer than the recurrence interval for strong earthquakes. It should also be taken into account that there is a certain area affected by landslides triggered by a single earthquake. Although there are a lot of factors, such as focal depth, specific ground motion characteristics of individual earthquake, geological conditions and so on, this area correlates with the earthquake magnitude and thus can be estimated (Keefer and Wilson 1989, Keefer 2002). Therefore, while calculating erosion rate, it should be compared in a proper way with studied area S (it is not possible to make correct calculations if studied area is smaller than the area affected by landsliding or only partially covers it). Thus, to quantify erosion due to seismically induced landslides, it is necessary to estimate the total volume of slope strata displaced as a result of all strong earthquakes within study area.

In case of modern, and more rarely, strong historic earthquakes, in-situ measurements are usually applied. Such a technique was utilized to study ground effects of the 1957 Gobi-Altai (M_W=8.1), the 1971 Oimjakon (M=6.9-7.0), the 1995 Tunka (M_S=5.9) and other earthquakes (Florensov and Solonenko 1965, Kurushin et al 1976, Agafonov 2002). The first step consists of mapping all triggered landslides. Then, an area of each seismically induced ground effect is measured in the field using detailed topographic maps, aerial photos, and GPS facilities. The volume could be calculated applying empirical correlations between the landslide area and its volume (for example those presented by Simonett (1967) [1] and Hovius et al (1997)[2]), geophysical methods (Havenith et al 2000) or, more often, by multiplying landslide area with the average thickness, usually estimated by the height of its front scarp.

When there is no possibility to apply geophysical techniques for determining subsurface geometry, to obtain more precise estimates of landform volume method of detailed profiling is often applied. This method is similar to the cross-sections technique in geodesy – each accumulated body is divided by profiles for separate prismatoids. Landslide bedrock topography is determined by morphology of undisturbed slope. Area of the prismatoid base is calculated on the basis of topographic or geodetic

[1] Correlation between landslide volume (V_L) and area (S_L) was obtained as a result of studying 201 landslides in New Guinea: $V_L = 0.024 \times S_L^{1.368}$

[2] Relationship $V_L = \varepsilon \times S_L^{1,5}$ (ε=0.05±0.02) was obtained on the basis of studying 4984 landslides in New Zealand.

data. Then calculated prismatoid volumes are summarized. Main difficulties associated with this technique include problems of clear identification of bedrock topography and separating different accumulative bodies in case of multiple landslide events. These difficulties are the main sources of errors.

Applying statistical methods is a completely different approach. Presence of representative statistical samplings gives an opportunity to establish correlations between different physical parameters (which characterize different aspects of seismic process and landslide event) without knowing the precise physical relationship between them [3]. Depending on landslide preservation, both analysis of historical inventory of seismically induced landforms (surface effects of several past seismic events within study area) and complete inventory of landslides associated usually with a single modern earthquake could be analyzed. By now the most exploitable relationship is the correlation between the total volumes of earthquake-triggered landslides V_{LT}, and the earthquake magnitude M[4], suggested by (Keefer and Wilson 1989). Later statistical sampling for regression and correlation analyses has been extended several times (Keefer 1994, Malamud et al 2004b). Now this correlation (equation 2) covers data on 17 modern earthquakes with instrumentally measured magnitude (Nepop and Agatova 2011) (Table 1, Figure 1).

$$\log V_{LT} = 1.39M - 10.95$$
$$(5.3 \le M \le 8.6;\ r^2 = 0.814;\ n = 17) \qquad (2)$$

[3] In this context *earthquake magnitude* as a measure of released seismic energy is preferable parameter. Being instrumentally measured it doesn't depend on experts. In contrast, *earthquake intensity* is an expert evaluation of damage and destructions within an area affected by seismic shock. Besides earthquake magnitude, *seismic moment* could be also applied. It is a measure of earthquake strength defined by shear modulus of the rocks involved in the earthquake, by area of the rupture along the geologic fault where the earthquake occurred, and by average displacement within this area.

[4] Here and below Moment Magnitude is implied and volumes measured in km^3, unless mentioned otherwise.

Despite different regional tectonic, climatic, geological and geomorphological settings for all presented earthquakes, there is a high correlation between the earthquake magnitude and the total volume of triggered landslides. Studying the complete inventory of landslides triggered by a single event, Malamud et al (2004a) calculated the general landslide probability distribution function. Using this function and equation (2) we correlated the total volume of earthquake-triggered landslides (V_{LT}) with the volume of the largest triggered mass movement V_{Lmax} (Nepop and Agatova 2011):

$$\log V_{LT} = 1.02 \log V_{L\max} + 0.89 \qquad (3)$$

Equations (2) and (3) give the opportunity to quantify total volumes of seismically displaced slope strata utilizing the magnitude of seismic shock or volume of the largest earthquake triggered landslide.

3 New Correlations for Estimating Earthquake Induced Topography Changes

The problem of correct magnitude determination is an obvious difficulty of applying equation 2

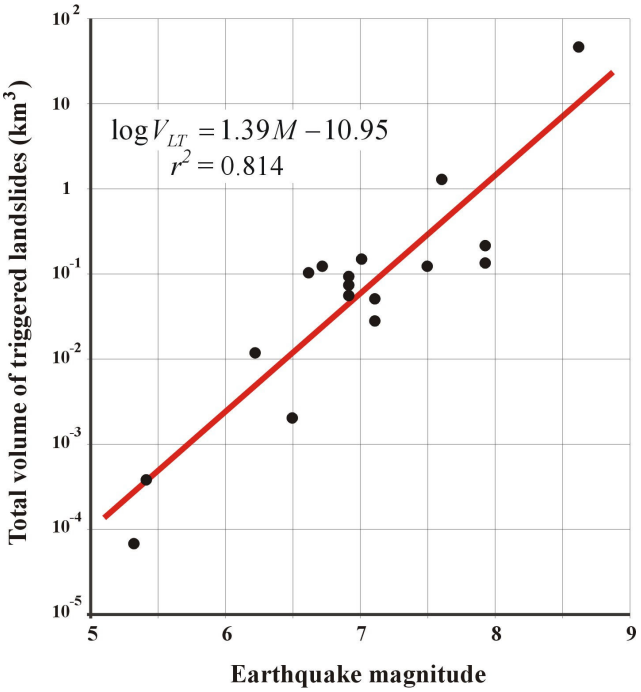

Figure 1. Correlation between total volume of triggered landslides and earthquake magnitude

for quantifying topographic changes induced by strong past earthquakes. In this case the largest

seismically triggered landslides could provide valuable information, first of all, due to their better preservation and then to their relation to the power of associated seismic events. Previously published equation 3 (Nepop and Agatova 2011) presents relationship between V_{LT} and V_{Lmax}. In this section, we suggest two new independent relations based on statistical approach. As a first step, utilizing data on 14 strong modern earthquakes with instrumentally measured magnitude (*M*) and estimated volume of the largest triggered landslide (V_{Lmax}), we calculated correlation between *M* and V_{Lmax} (see correlation graph in Figure 2, based on data included in Table 2):

$$M = 0.78 \times \log V_{L\max} + 8.34,$$
$$(4.9 \le M \le 8.1;\ r^2 = 0.862;\ n = 14) \qquad (4)$$

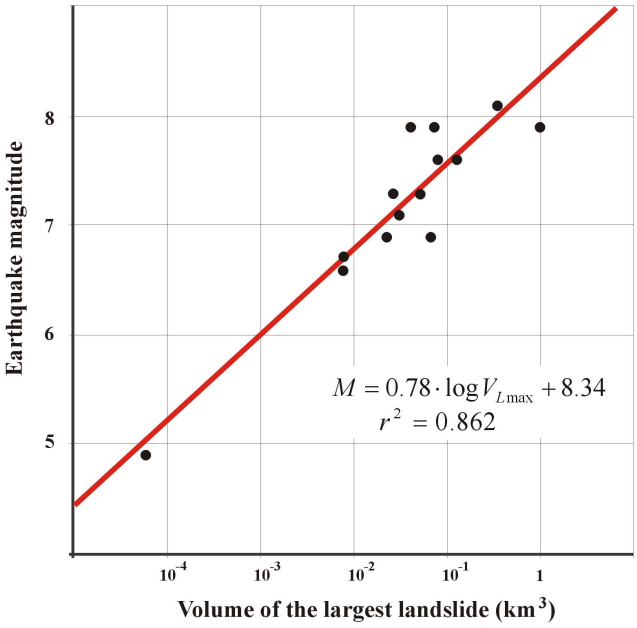

Figure 2. Correlation between earthquake magnitude and the volume of largest triggered landslide

Table 1. Earthquake location, date and moment magnitude M, along with corresponding volume V_{LT} associated with the earthquake

Location	Date	*M*	V_{LT} (km^3)	Reference
Arthur's Pass, New Zealand	09.03.1929	6,9	0,059	Adams 1980
Buller, New Zealand	17.06.1929	7,6	1,3	Adams 1980
Torricelli Mtns., New Guinea	20.09.1935	7,9	0,215	Simonett 1967
Assam, India	15.08.1950	8,6	47	Mathur 1953
Daily City, CA, USA	22.03.1957	5,3	0,000067	Bonilla 1960
Inangahua, New Zealand	23.05.1968	7,1	0,052	Adams 1980
Peru	31.05.1970	7,9	0,141	Plafker et al 1971
Papua New Guinea	31.10.1970	7,1	0,028	Pain and Bowler 1973
Guatemala	04.02.1976	7,6	0,116	Harp et al 1981
Darien, Panama	11.07.1976	7	0,13	Garwood et al 1979
Mammoth Lakes, CA, USA	25.05.1980	6,2	0,012	Harp et al 1984
Coalinga, CA, USA	02.05.1983	6,5	0,00194	Harp and Keefer 1990
San Salvador, El Salvador	10.10.1986	5,4	0,000378	Rymer 1987
Ecuador	05.03.1987	6,9	0,0925	Evans and DeGraff 2002
Loma Prieta, CA, USA	17.10.1989	6,9	0,0745	Keefer 1989
Northridge, CA, USA	17.01.1994	6,7	0,12	Harp and Jibson 1996
Niigata, Japan	23.10.2004	6,6	0,1	Guidebook 2008

Table 2. Earthquake location, date and moment magnitude M, along with corresponding volume V_{Lmax} associated with the earthquake

Location	Date	*M*	V_{Lmax} (km^3)	Reference
Gobi-Altai, Mongolia	04.12.1957	8,1	0,342	Florensov and Solonenko 1965
Peru	31.05.1970	7,9	0,075	Stephen et al 2002
Irpinia, Italy	23.11.1980	6,9*	0,023	Porfido et al 2002
Racha earthquake, Georgia	29.04.1991	7,1	0,03	Jibson et al 1994
Suusamyr earthquake, Kirgizia	19.08.1992	7,3*	0,05	Havenith 2008
Northridge, CA, USA	17.01.1994	6,7	0,008	Harp and Jibson 1996
Chi-Chi earthquake, Taiwan	21.09.1999	7,6	0,125	Lee 2000
Denali earthquake Alaska, USA	03.11.2002	7,9	0,04	Harp et al 2003
Chuya earthquake, Russia	27.09.2003	7,3	0,027	Nepop and Agatova 2008
Niigata, Japan	23.10.2004	6,6	0,0075	Hasbaator et al 2006
Kashmir earthquake, Pakistan	08.10.2005	7,6	0,08	Owen et al 2008
Handiza earthquake, Uzbekistan	25.04.2008	4,9	0,00006	Nijazov and Nurtaev 2009
Sichuan earthquake, China	12.05.2008	7,9	1	Chigira and Woo 2008
Iwate-Miyagi, Japan	14.06.2008	6,9	0,067	Tohoku Regional Bureau of MLIT 2008

*Magnitude of surface waves is presented

If regional geologic evidences argue for invariability of seismic regime within study area, this relationship allows estimating magnitudes of paleoearthquakes, which is important for assessing earthquake hazard and seismic risk zoning. Applying equations 2 and 4 also allows calculating relation between V_{LT} and V_{Lmax} in another way (different from equation 3):

$$\log V_{LT} = 1.08 \times \log V_{L\max} + 0.64 \qquad (5)$$

Studying general properties of the statistical landslide probability distribution function, Malamud et al (2004a) present a number of quantitative relationships between physical parameters, which characterize a complete inventory of these landforms (equations 4 - 9 in (Malamud et al 2004a)[5]). Using equations 7 and 9 from that paper, relation between V_{LT} and V_{Lmax} could be calculated by another different method:

$$\log V_{LT} = 1.048 \log V_{L\max} + 0.876 \qquad (6)$$

Thus application of statistical approach allows calculating the total volume of landslides triggered by a single earthquake using information about the largest landslide (equations 3, 5 and 6). To quantify erosion rate due to seismically triggered landslides applying relationship (1), first of all, the largest earthquake induced landslides for a particular area should be

[5] $\overline{S}_L[km^2] = \int_0^\infty S_L \times \rho(S_L) \times dS_L = 3.07 \times 10^{-3}$

$\overline{V}_L[km^3] = (7.3 \times 10^{-6}) \times N_{LT}^{0.122}$

$S_{LT}[km^2] = \overline{S}_L \times N_{LT} = (3.07 \times 10^{-3}) N_{LT}$

$V_{LT}[km^3] = \overline{V}_L \times N_{LT} = (7.3 \cdot 10^{-6}) \times N_{LT}^{1.122}$

$S_{L\max}[km^2] = (1.10 \times 10^{-3}) N_{LT}^{0.714}$

$V_{L\max}[km^3] = (1.82 \times 10^{-6}) \times N_{LT}^{1.071}$

here N_{LT} - number of landslides in complete inventory; $\overline{S}_L$, $\overline{V}_L$ - average area and volume; S_{LT}, $S_{L\max}$ - total area of landslides and an area of the largest landslide; $\rho(S_L)$ - probability density function.

detected. Accumulative bodies of these landforms should be delineated for estimating their areas and further calculating landslide volumes by methods suggested above. Obvious advantage of statistical approach in comparison with in-situ measurements is taking into account the volumes of not only the largest landforms but the volumes of all triggered landslides including even smaller ones that are completely destroyed during the time and are not identified in topography. Thus for calculating correlation (2), modern earthquakes with complete inventory of triggered landslides (including the smaller ones) were studied, and for establishing correlations (3) and (6), general landslide probability distribution function (which does not "lose" smaller landslides) was additionally applied.

The main difficulty in calculating erosion due to seismically induced landslides on the basis of statistical approach is determining the characteristic sizes of the largest landslides triggered by earthquakes of specific magnitude for studied area. Due to the fact that weak seismic events can generate the largest landslides comparable in size with "ordinary" landslides triggered by strong earthquake, it is necessary to detect particularly the largest landslides within the study area taking into account their age and state of preservation.

It should be also mentioned that all presented correlations were calculated for earthquakes that triggered the largest landslide with an area of accumulative body no more than 1 km^2. Application of obtained relations for studying much larger seismically induced landforms actually needs a separate investigation.

4 Application of the Suggested Approach in the SE Altai

4.1 Study area

The above suggested approach of quantitative estimation of the Holocene erosion due to seismically induced landslides was applied in the course of the paleoseismicity study of the southeastern part of Russian Altai (SE Altai) (Figure 3). This is the highest part of Russian

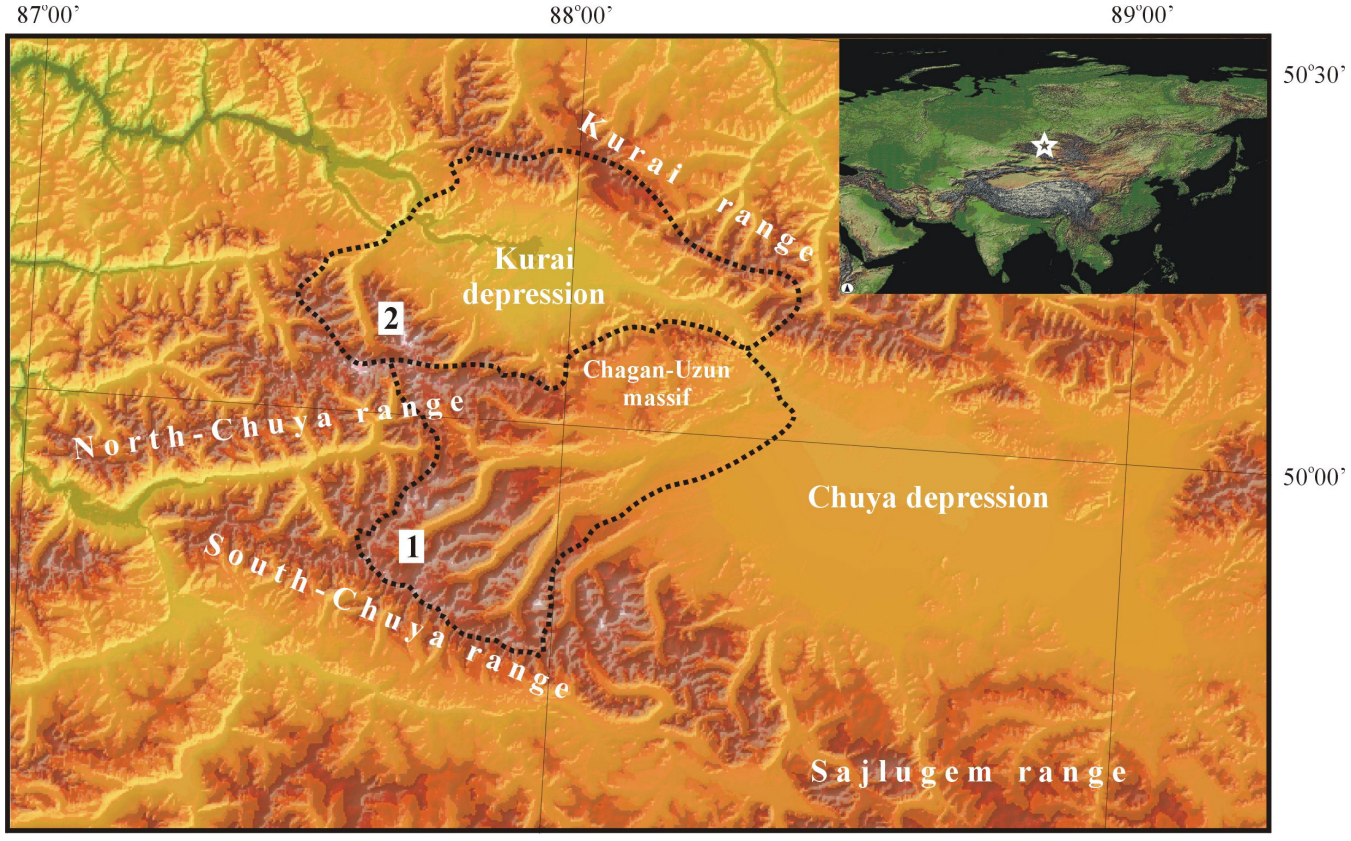

Figure 3. Study area. Location of the SE Altai within the Altai Mountains. Dotted lines show the boundaries of 1) the Chagan-Uzun river basin, and 2) Kurai basin.

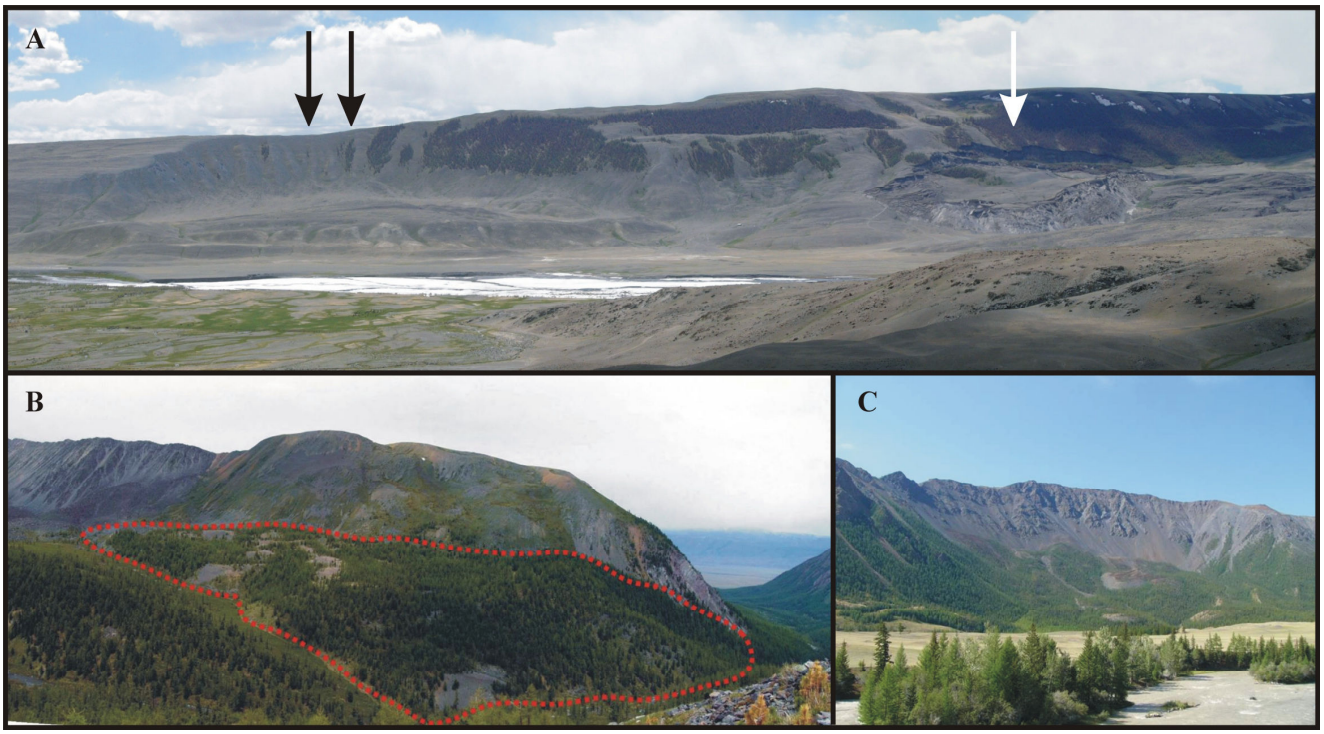

Figure 4. Some giant earthquake triggered landslides within the study area. A – Taldura river valley, black arrows show ancient landslide and white arrow – the largest landslide triggered by the 2003 Chuya earthquake; B – Tjute valley; C – the largest in the SE Altai multievent Sukor seismogravitational paleodislocation

Altai with most strongly dissected topography which is characterized by extremely arid climate. The Altai neotectonic uplift is the northern part of the Central-Asian collision belt and is a transpressional zone formed due to oblique thrusting. The southeastern part of Russian Altai is the northern extension of the Mongolian Altai, which is known for its high seismicity. As a result, SE Altai is the most seismically active part of Russian Altai. This was evidenced by the 2003 Chuya earthquake (M_S=7.3), which triggered giant (for Russian Altai) landslide in Taldura valley (Figure 4).

The historical chronicles which mentioned strong earthquakes in the SE Altai are quite poor, seismostatistical database is quite limited, and period of seismological regional studies is short (regional seismological network was developed in 1962). Along with old ruptures, the only evidence of the high Holocene regional seismicity is provided by the giant earthquake-induced paleolandslides (Figure 4). Kurai-Chuya system of intermountain depressions and framing ridges is the most ancient area of orogenesis within Altai Mountains uplift (Devyatkin 1965, Bogachkin 1981), and is still active during the Holocene. The recurrence interval of strong earthquakes here is about 500 - 900 years in the Holocene (Rogozhin et al 2007) and about 400 years during the last 4000 years (Agatova and Nepop 2016). Ground effects of a series of strong past earthquakes, which struck this mountain province after degradation of the Late Pleistocene glaciations, are clearly identified in the topography (Butvilovsky 1993, Rogozhin and Platonova 2002, Novikov 2004, Agatova et al 2006, Rogozhin et al 2007, Nepop and Agatova 2011). The 2003 Chuya earthquake (M_S=7.3) is the latest in this series.

Unconsolidated Cenozoic sediments are widely distributed in the region in the most active areas at the depression-range transition along fault boundaries of landforms and provide geological conditions to produce earthquake induced landslides. All studied giant landslides evidently have Late Pleistocene - Holocene ages because the youngest displaced rocks are Late Pleistocene moraine and glaciofluvial deposits that cover the valleys at the depression-range transition. Several radiocarbon dates of associated

sediments were obtained for some giant earthquake triggered landslides within the Chagan-Uzun river basin, SE Altai (Rogozhin et al 2008, Agatova and Nepop 2016). The oldest among them (8100±410 IGAN 3211 (Rogozhin et al 2008)) also supports this thesis. A few papers (Butvilovsky 1993, Rogozhin and Platonova 2002) present approximate estimations of the volumes of some earthquake triggered paleolandslides. But erosion due to seismically induced landslides for Russian Altai has not been estimated previously.

The Chagan-Uzun river basin (surface area ≈1430 km^3, see Figure 3) was chosen as a key area which represents earthquake impact on topographic changes. A number of giant seismically induced paleo-landslides was mapped here (Agatova et al 2006, Rogozhin et al 2008, Nepop and Agatova 2011). Study area includes southwestern part of Chuya intermountain depression, framing (South Chuya and North Chuya) ranges, and the part of Chagan-Uzun massif. This massif is a single neotectonic block, which separates Chuya and Kurai intermountain depressions. Faults bordering this block are some of the most active seismogenerative structures within the SE Altai, and are marked by the presence of the largest earthquake induced landslides. Rock composition of the Chagan-Uzun massif plays its role in the uplifting of this block. That is first of all serpentinized peridotite which produce numerous glide planes within fault zones.

Erosion due to seismically induced landslides estimated for the Chagan-Uzun river basin on the basis of statistical approach and in-situ measurements was compared with those calculated for the neighboring Kurai basin which has a comparable area ≈1660 km^2 (Figure 3). Apart from western part of the Chran-Uzun massif, Kurai and North Chuya ranges, this basin includes exposures of the Paleozoic basement, which according to Rogozhin and Platonova (2002) and Novikov (2004), represent denuded parts of the floor of Kurai intermountain depression as well as the Cenozoic sedimentation basin in its eastern part. The area ratio of strongly dissected mountain parts of the basin and steeply inclined slightly dissected plain parts (without any traces of landsliding) is 2.6 for the Kurai basin (1200 km^2 and 460 km^2, respectively) and 6.5 for the Chagan-Uzun river basin (1240 km^2 and 190 km^2, respectively).

It should be mentioned that generally all types of landslides triggered by earthquakes may also occur without seismic triggering (Jibson 1996, Keefer 2002). Strong earthquakes are the leading factor in the generation of giant landslides in the SE Altai. Our field observations of the impact of strong modern and prehistoric earthquakes reveal several criteria that indicate seismic origin of observed ground failures within studied area (Nepop and Agatova 2008): *i*) the great extent of ground failures upon strongly cemented Neogene and Pleistocene permafrost sediments, as well as high concentration of numerous seismically induced landforms (both huge and small ones) within the same area; *ii*) location of the landslides in the most active areas at the basin-range transition along fault boundaries of landforms and fault crossings; *iii*) absence of correlation between location of landslides and exposure of slopes to insolation, their age and rock composition; and *iiii*) conjunction (relative position) of landslide locations with the ruptures on the watersheds and valley slopes. It should be also noted that location of all giant landslides in an area of extremely dry climate with 100 - 200 mm mean annual precipitation in the floor of the Chuya intermountain depression (Bulatov et al 1967) rules out their rainfall or a snowmelt trigger. While quantifying erosion due to seismically induced landslides, only strong earthquakes were taken into consideration. This approach is quite reasonable because of the much more significant influence of strong earthquakes on mountain topography in comparison with the moderate seismic shocks. As evidenced by the example of the 1995 Tunka earthquake (M=5.9), the volume of eroded material as a result of moderate seismic shock is two orders of magnitude less than those produced by strong earthquakes (Agatova and Nepop 2011).

4.2 Quantitative estimates of erosion due to seismically induced landslides on the basis of statistical approach

As it was mentioned above, the main difficulty in applying a statistical approach is determining the

typical size of the largest earthquake triggered landslides for studied area. To date, there are no special studies of statistical distribution of seismically induced landslide in Russian Altai. Nevertheless, the difference in volumes of the largest and other landslides triggered by the 2003 Chuya earthquake is at least two orders of magnitude. Taking into account the constancy of seismic regime and similarity of mechanisms of seismic excitations within study area during the Holocene (Agatova and Nepop 2009, 2011), it could be suggested that each of the large ancient landslides that is comparable in size with the largest landslide triggered by the 2003 Chuya earthquake indicates a separate strong past seismic event.

For calculating erosion due to seismically triggered landslides in the Chagan-Uzun river basin, we utilized the volumes of the largest landslides mapped there together with the data on the 2003 Chuya earthquake. Surface effects of this recent strong seismic event were estimated applying equation (2). Landslide accumulative bodies were contoured by GPS navigator and surface areas were measured in ArcView GIS 3.2 software using topographical maps, scale 1:25000. Landslide volumes were calculated applying empirical correlations presented in Hovius et al (1997).

Using all obtained correlations between total volumes of landslides generated during seismic excitation and volume of the largest triggered landslide (equations 3, 5 and 6) we quantified total volumes of displaced slope strata (2.50×10^{-1}, 3.58×10^{-1}, 3.34×10^{-1} km^3) and the Holocene erosion rate due to seismically induced landslides for the Chagan-Uzun river basin (equation 1) – 2.1×10^{-5}, 3.0×10^{-5}, 2.8×10^{-5} m a^{-1} respectively. All these values have the same order of magnitude.

The marginal error of these calculations can be estimated assuming that each of mapped earthquake induced landslides regardless of its size is the largest landslide triggered by separate seismic event. In this assumption overestimated erosion will be 5.4×10^{-5} m a^{-1}, about two times greater than calculated one, and will have the same order of magnitude.

Another difficulty while quantifying erosion can occur when accumulative landslide bodies of the second and even the third generations are concentrated practically on the same area and sometimes overlie each other. That is a typical situation in the SE Altai where during the Holocene the same focal zones have been repeatedly reactivated. In this case the suggested approach allows more precise estimates of parameters of the youngest triggered landslide. At the same time while estimating the total volume of earthquake induced landslides using equations 3, 5 and 6, the error caused by wrong number of determined events doesn't exceed 5 %, which can be ignored (three landslides with the volume of $V_{Lmax}/3$ were used instead of one with V_{Lmax}).

Among other problems of applying the suggested technique some local difficulties in establishing the seismic origin of landslide events and determining of the landslide parameters should be mentioned, as well as problems of absolute age determination of paleolandslides. These difficulties are typical for paleoseismogeological investigations and are discussed in the literature (see McCalpin 2009 for the most complete recent overview).

4.3 Quantitative estimates of erosion due to seismically induced landslides on the basis of detailed profiling of landslides

In addition to application of statistical approach, estimating the volumes of all mapped landslides within study area was carried out utilizing detailed profiling technique (Figure 5). For this purpose, interpretation of aerial photographs and extensive field investigations were carried out in order to mark all seismically induced landforms. The calculated total volume of earthquake triggered landslides in Akkol, Chagan, Kuskunur river valleys (Chagan-Uzun river basin) is 1.33×10^{-1} km^3 and the Holocene erosion rate for the Chagan-Uzun river basin is 1.1×10^{-5} m a^{-1}. This value is lower than erosion rate calculated on the basis of statistical approach. It can be explained by decreasing volumes of landslides that are affected by erosion as well as by destruction over the time of small landforms. Nevertheless, calculated values have the same order of magnitude.

Total volumes of the Holocene earthquake-

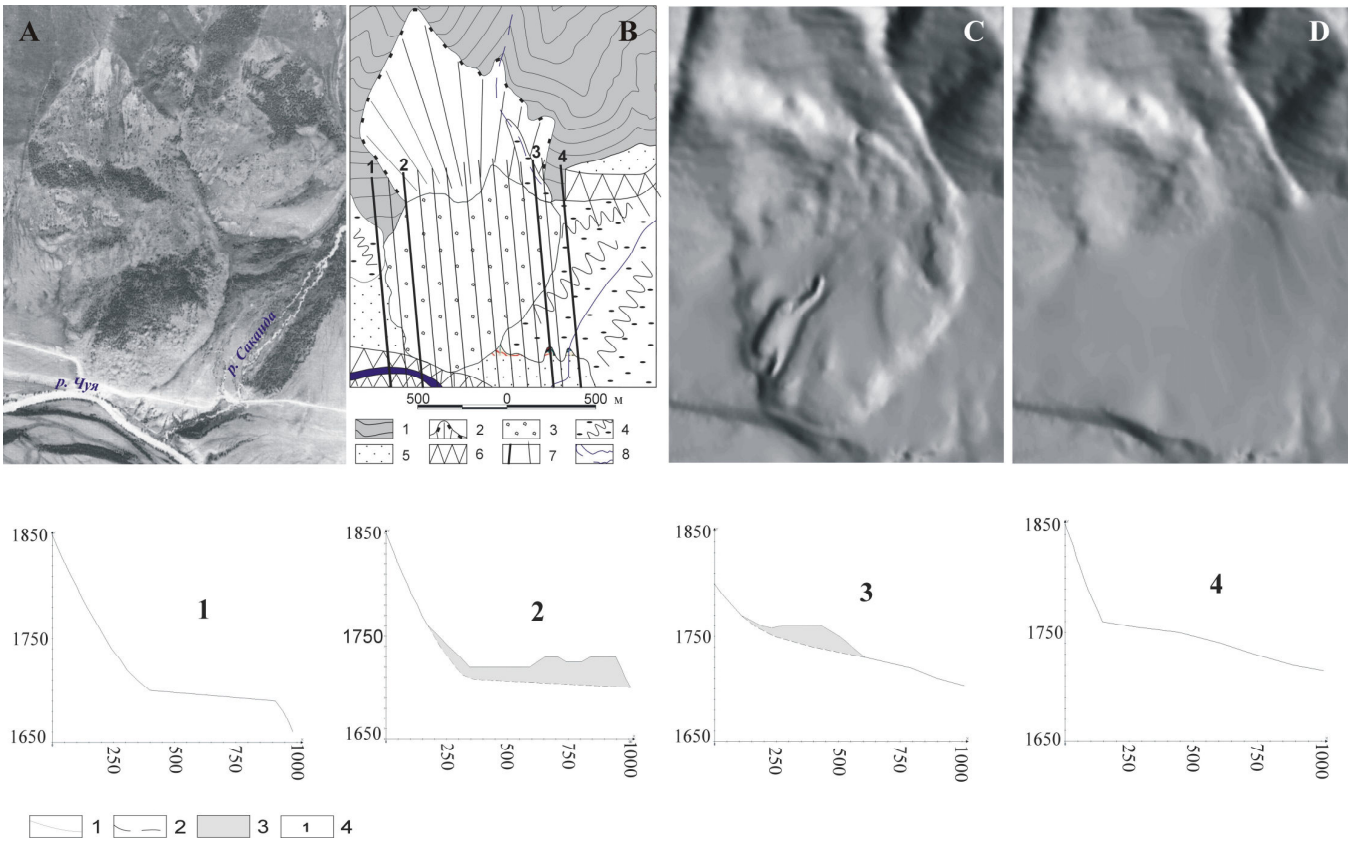

Figure 5. Method of detailed profiling. Earthquake triggered landslide near the Sakanda river, Kurai basin. A – aerial photograph; B – geomorphological map (1- valley slopes, 2- main scarp, 3- landslide body, 4- proluvial fans, 5- terrace, 6- terrace's brows, 7- profiles, 8- rivers); C – digital elevation model; D – the same model without landslide; numbers 1-4 show corresponding profiles (1- relief, 2- landslide bedrock, 3- accumulative body, 4- profile number)

triggered landslides within the neighboring territory of the Kurai basin and framing ridges, which was calculated applying the same technique is 2.25×10^{-1} km^3. The major volumes of slope colluvium of seismic origin are concentrated in Kuektanar, Tute, Arydjan, and Chuya (between Chuya and Kurai intermountain depressions) river valleys, which support modern seismotectonic activity of the Chagan-Uzun massif. Calculated the Holocene erosion rate due to seismically induced landslides in this part of the SE Altai is 1.4×10^{-5} m a^{-1}, which is practically equal to this rate in the Chagan-Uzun river basin.

Thus the Holocene erosion rate due to seismically induced landslides obtained by applying different techniques can be estimated as $(1.1\text{-}3.0) \times 10^{-5}$ m a^{-1}. This assessment characterizes erosion within the Chuya-Kurai system of intermountain depressions and their framing ridges more precisely because of the similarity of geomorphological and climatic conditions. Lower rates of erosion can be expected in the southeastern part of studied area within significantly less dissected northern slopes of the Sajlugem range. At the same time the fault boundary between South Chuya and Sajlurem ranges along the Tarkhata river valley is marked by numerous earthquake induced landslides.

5 Conclusion

Estimating earthquake magnitudes and earthquake-induced topography changes using instrumental data and historic accounts can give information about the seismicity of mountain provinces during a relatively short time period. Analysis of geomorphically expressed surface displacements of obviously seismic origin can provide valuable information about regional

paleo-seismicity. So far most of the research was focused on coseismic fault motion. Giant earthquake-triggered landslides have been used mainly for establishing epicentral zones and the timing of old earthquakes. At the same time using the parameters of the largest seismically induced landslides for estimating earthquake magnitudes and earthquake induced topographic changes can improve the analysis of seismotectonic dislocations.

The new relationship between earthquake magnitude and the volume of the largest triggered landslide, the correlation between earthquake magnitude and total volume of triggered landslides, as well as previously published general landslide probability distribution functions allow us to calculate correlations between the total volumes of slope strata displaced by strong earthquake and the volume of the largest triggered landslide. The presented equations allow us to quantify erosion due to seismically induced landslides.

The suggested approach was tested in the course of a paleo-seismogeological study of the most active high-mountainous SE Altai, which is characterized by an arid climate. Total volume of slope material displaced during past earthquakes within the Chagan-Uzun river basin, which was calculated on the basis of statistical correlations, is $(3.0\text{-}4.3)\times10^{-1}$ km^3, and the Holocene erosion rate due to seismically induced landslides $(1.1\text{-}3.0)\times10^{-5}$ m a^{-1}. These estimates were certified by calculating the volumes of earthquake triggered landslides within the Chagan-Uzun river basin and neighboring Kurai basin on the basis of detailed profiling approach. The estimated volumes of seismically displaced slope strata are 1.33×10^{-1} and 2.25×10^{-1} km^3, and the Holocene erosion rate 1.1×10^{-5} and 1.4×10^{-5} m a^{-1}, respectively.

Thus the Holocene erosion rate due to seismically triggered landslides in the SE Altai calculated by two different methods could be defined as $(1.1\text{-}3.0)\times10^{-5}$ m a^{-1} and most precisely characterizes this process within the Chuya-Kurai system of intermountain depressions. Quantitative assessment of erosion due to earthquake induced landslides indicates that together with the glacial and fluvial activity it is one of the major relief changing processes in the SE Altai and forms about 10% of the total regional denudation in the Holocene.

Difficulties associated with this approach suggest some numerical estimates of possible errors. However, the quantitative values obtained are the most precise indicators of the order of magnitude of the intensity of the studied processes reported to date. Taking into account the complexity of the problem of paleo-environmental reconstructions it is an acceptable result.

The suggested approach expands the scope of classical paleo-seismogeological methods and allows quantifying erosion due to seismically induced landslide for seismically active mountain provinces where historical chronicles are not available, period of instrumental seismological observations is short, and giant earthquake triggered paleo-landslides are the major evidences of strong past seismic events.

Acknowledgement

A.F. Emanov, the head of the Altai-Sayan branch of the Geophysical survey SB RAS, is kindly thanked for his assistance in organizing of field research. We are grateful to Professor Olav Slaymaker for constructive comments and suggestions that strengthened manuscript and made it more clear. The study was partially funded by Russian Foundation for Basic Researches (grants 15-05-06028, 16-05-01035).

References

Agafonov, B.P., 2002. Tectonically fractured slopes in areas of active faults - sensitive indicators of moderate seismic impact. Volcanology and seismology, **1**: 61 - 71. (in Russian).

Agatova, A.R., R.K. Nepop and E.M. Vysotsky, 2006. Seismogravitational paleodislocations in the Chagan-river valley (SE Altai). Geomorfologiya, **4**: 53 - 62. (in Russian).

Agatova, A.R. and R.K. Nepop, 2009. Estimating the contribution of aftershock-induced landslides to seismo-gravitational denudation (by the example of the 2003 Chuya

Earthquake). Geomorfologiya, **4**: 53 - 63. (in Russian).

Agatova, A.R. and R.K. Nepop, 2011. Assessing the rate of seismogravitational denudation of the relief of Southeastern Altai: The Chagan_Uzun R. Basin. Journal of Volcanology and Seismology, **5**(6): 53 - 62.

Agatova, A.R. and R.K. Nepop, 2016. Dating strong prehistoric earthquakes and estimating their recurrence interval applying radiocarbon analysis and dendroseismological approach – case study from SE Altai (Russia). This special issue.

Adams, J., 1980. Contemporary uplift and erosion of the Southern Alps, New Zealand. Geological Society of America Bulletin, **91**(2): 1 - 114.

Bogachkin, B.M., 1981. History of Cenozoic Tectonic Evolution of Gorny Altai. Moscow: Nauka. 132p. (in Russian).

Bommer, J.J and C.E. Rodriguez, 2002. Earthquake-induced landslides in Central America. Engineering Geology, **63**: 189 - 220.

Bonilla, M.G., 1960. Landslides in the San Francisco South Quadrangle, California. U.S. Geological Survey Open-File Rep.

Bulatov, V.I., I.P. Dik and V.S. Revjakin, 1967. Glaciological observations in Akkol-river basin. Glyatsiologiya Altaya, **5**: 178 - 183. (in Russian).

Butvilovsky, V.V., 1993. Paleogeography of the Last Glaciation and the Holocene of Altai: a catastrophic events model. Tomsk University Press, Tomsk. 253p. (in Russian).

Chigira, M. and X. Woo, 2008. Takashi Inokuchi Landslides Induced by the 2008 Wenchuan Earthquake, Sichuan in China. Proceedings of the First World Landslide Forum, United Nations University, Tokyo, Japan, 149 - 150.

Devyatkin, E.V., 1965. Cenozoic sediments and neotectonics of the SE Altai, USSR Academy of Science, Moscow, (GIN Transactions, Issue 126), 244p. (in Russian).

Evans, S.G. and J.V. DeGraff, 2002. Catastrophic landslides: effects, occurrence, and mechanisms. Geological Society of America, 411p.

Florensov, N.A. and V.P. Solonenko, 1965. The Gobi-Altai Earthquake, US department of Commerce, DC. 424p.

Garwood, N.C., D.P. Janos and N. Brokaw, 1979. Earthquake caused landslides: a major disturbance to tropical forests. Science, **205**: 997 - 999.

Guidebook for Trans-TOHOKU Field Trip on landslides, 2008. International Conference on Management of Landslide Hazard in Asia-Pacific Region, Tohoku Gakuin University, Sendai, Japan.

Iveronova, M.I., 1969. Quantitative analysis of the process of modern denudation. Proceedings of Russian Academy of Sciences. Series Geographical, **2**: 13 - 24. (in Russian).

Harp, E.L. and R.W. Jibson, 1996. Landslides triggered by the 1994 Northridge, California, Earthquakes. Bulletin of the Seismological Society of America, **86**(1B): S319 - S332.

Harp, E.L. and D.K. Keefer, 1990. Landslides triggered by the earthquake. In: Rymer, M.J. and Ellsworth, W.L. (eds.), The Coalinga, California, Earthquake of May 2, 1983. U.S. Geological Survey Professional Paper, 335 - 347.

Harp, E.L., K. Tanaka, J. Sarmiento and D.K. Keefer, 1984. Landslides from the May 25 - 27, 1980, Mammoth Lakes, California, earthquake sequence. U.S. Geological Survey Misc. Invest. Ser. Map. 1 - 1612.

Harp, E.L., R.W. Jibson, R.E. Kayen, D.K. Keefer, B.L. Sherrod, G.A. Carver, B.D. Collins, R.E.S. Moss and N. Sitar, 2003. Landslides and liquefaction triggered by the M 7.9 Denali fault earthquake of 3 November 2002. GSA today, **13**(8): 4 - 10.

Harp, E.L., R.C. Wilson and G.F. Wieczorek, 1981. Landslides from the February 4, 1976, Guatemala Earthquake. U.S. Geological Survey Professional Paper 1204-A.

Hasbaator, M., Hanaoka, E. Nozawa, A. Momose and K. Sasaki, 2006. Behavior and mechanism of earthquake-induced landslides within pre-existed landslide topography, the case of 2004 Mid Niigata Prefecture Earthquake, Japan. Proceedings of the International Symposium Disaster Mitigation of Debris Flows, Slope Failures and Landslides, Universal Academy Press. Inc. Tokyo, Japan, 35 - 46.

Havenith, H.B., 2008. Landslides triggered by

earthquakes in the Tien Shan: a review and a (problematic) case study. Proceedings of the International Conference on Management of Landslide Hazard in Asia-Pacific Region, Tohoku Gakuin University, Sendai, Japan, 175 - 186.

Havenith, H.B., D. Jongmans, K. Abdrakhmatov, P. Trefois, D. Delvaux and I.A. Torgoev, 2000. Surveys in Geophysics, **21**: 349 - 369.

Havenith, H.B., A. Strom, I. Torgoev, A. Torgoev, L. Lamair, A. Ischuk and K. Abdrakhmatov, 2015. Tien Shan geohazards database: earthquakes and landslides. Geomorphology, **249**: 16 - 31.

Hovius, N, C.P. Stark and P.A. Allen, 1997. Sediment flux from a mountain belt derived by landslide mapping. Geology, **25**: 801 - 804.

Jibson, R.W., 1996. Use landslides for paleoseismic analysis. Engineering Geology, **43**: 291 - 323.

Jibson R.W., C.S. Prentice, B.A. Borissoff, E.A. Rogozhin and C.J. Langer, 1994. Some observations of landslides triggered by the 29 April 1991 Racha earthquake, Republic of Georgia. Bulletin Seismological Society of America, **84**(4): 963 - 973.

Kashiwaya, K., Y. Tsuya and T. Okimura, 2004. Earthquake-related geomorphic environment and pond sediment information. Earth Surface Processes and Landforms, **29**: 785 - 793.

Keefer, D.K., 1989. The Loma Prieta, California, Earthquake of October 17, 1989. U.S. Geological Survey Professional Paper, 1551-C.

Keefer, D.K., 1994. The importance of earthquake-induced landslides to long-term slope erosion and slope-failure hazards in seismically active regions. Geomorphology, **10**: 265 - 284.

Keefer, D.K., 2002. Investigating landslides caused by earthquakes – a historical review. Surveys in Geophysics, **23**: 473 - 510.

Keefer, D.K. and R.C. Wilson, 1989. Predicting earthquake-induced landslides, with emphasis on arid and semi-arid environments. Landslides in Semi-Arid Environments with Emphasis on Inland Valleys of Southern California, Inland Geological Society of Southern California Publications, Riverside, CA, **2**(1): 118 - 149.

Kurushin, R.A., M.G. Demjanovich and V.M. Kochetkov, 1976. Macroseismic effects of the Oimjakon earthquake. Seismicity and deep structure of Siberia and Far East, Vladivostok: DVNC Publisher, 50 - 60. (in Russian)

Lee, S.W., 2000. CHI-CHI earthquake and debris disasters. J. Jpn. Landslide Soc., **37**(1): 51 - 59.

Malamud, B.D., D.L. Turcotte, F. Guzzetti and P. Reichenbach, 2004a. Landslides inventories and their statistical properties. Earth Surface Processes and Landforms, **29**: 687 - 711.

Malamud, B.D., D.L. Turcotte, F. Guzzetti and P. Reichenbach, 2004b. Landslides, earthquakes and erosion. Earth and Planetary Science Letters, **229**: 45 - 59.

Mathur, L.P., 1953. Assam earthquake of 15th Aug., 1950 - a short note on factual observations. Compilation of Papers on the Assam Earthquake of August 15. 1950. National Geophysical Research Institute, Hyperabad, India.

McCalpin, J.P., 2009. Paleoseismology. 2nd edition. Elsevier, San Diego.

Nepop, R.K. and A.R. Agatova, 2008. Estimating magnitudes of prehistoric earthquakes from landslide data: first experience in southeastern Altai. Russian Geology and Geophysics, **49**(2): 144 - 151.

Nepop, R.K. and A.R. Agatova, 2011. Numerical estimating of erosion due to seismically induced landslides by the example of the SE Altai. Lithosphere, **2**: 111 - 121. (in Russian).

Nijazov, R.A. and B.S. Nurtaev, 2009. Landslides in Uzbekistan occurred during earthquakes of Pamir-Hindikush area. Mitigation of Natural Hazards in Mountain Areas. Tuzova, T.V. (ed.), Bishkek: Salam, 139 - 142.

Novikov, I.S., 2004. Morphotectonic of Altai. SB RAS Geo, Novosibirsk, 313p. (in Russian).

Owen, L.A., U. Kamp, G.A. Khattak, E.L. Harp, D.K. Keefer and M.A. Bauer, 2008. Landslides triggered by the 8 October 2005 Kashmir earthquake. Geomorphology, **94**(1): 1 - 9.

Pain, C.F. and J.M. Bowier, 1973. Denudation following the November 1970 earthquake at Magang, Papua New Guinea. Geomorphology, **18**: 92 - 104.

Plafker, G., G.E. Ericksen and J. F. Concha, 1971.

Geological aspects of the May 31, 1970, Peru earthquake. Bulletin of the Seismological Society of America, **61**: 543 - 587.

Porfido, S., E. Esposito, E. Vittori, G. Tranfaglia, A.M. Michetti, M. Blumetti, L. Ferreli, L. Guerrieri and L. Serva, 2002. Areal distribution of ground effects induced by strong earthquakes in the Southern Apennines (Italy). Surveys in Geophysics, **23**: 529 - 562.

Rogozhin, E.A. and S.G. Platonova, 2002. Strong earthquake focal zones of Gorny Altai in the Holocene. UIPE RAS, Moscow, 130p. (in Russian).

Rogozhin, E.A., A.N. Ovsyuchenko, A.V. Marahanov and E.A. Ushanova, 2007. Tectonic setting and geological manifestations of the 2003 Altai earthquake. Geotectonics, **47**(2): 87 - 104.

Rogozhin, E.A., A.N. Ovsyuchenko and A.V. Marahanov, 2008. Major earthquakes of the southern Gorny Altai in the Holocene. Izv. Physics Solid Earth, **44**(6): 469 - 486.

Rymer, M.J., 1987. The San Salvador earthquake of October 10, 1986 - geologic aspects. Earthquake Spectra, **3**: 435 - 463.

Schuster, R.L. and L.M. Highland, 2001. Socioeconomic and environmental impacts of landslides in the western hemisphere, USGS Open-File Report, 1 - 276.

Simonett, D.S., 1967. Landslide distribution and earthquakes in the Bewani and Torricelli Mountains, New Guinea - a statistical analysis. Landform Studies from Australia and New Guinea. Cambridge Univ. Press, Cambridge.

Solonenko, V.P., 1962. Establishing eartquake's epicentral zones from geological evidences. Bulletin of the USSR Academy of Sciences. Geology, **11**: 58 - 74. (in Russian).

Solonenko, V.P., 1973. Earthquakes and relief. Geomorfologiya, **4**: 3 - 13. (in Russian).

Tohoku Regional Bureau of MLIT: Leaflet on the Iwate Miyagi Nairiku earthquake 2008. Ministry of Land, Infrastructure, Transport and Tourism. 2008. 46p. (in Japanese).